HIPPOCAMPUS 22:1379–1391 (2012)

Extrinsic and Local Glutamatergic Inputs of the Rat Hippocampal CA1 Area Differentially Innervate Pyramidal Cells and Interneurons

Virág T. Takács,[1*] Thomas Klausberger,[2,3] Peter Somogyi,[1,2,3] Tamás F. Freund,[1] and Attila I. Gulyás[1]

ABSTRACT: The two main glutamatergic pathways to the CA1 area, the Schaffer collateral/commissural input and the entorhinal fibers, as well as the local axons of CA1 pyramidal cells innervate both pyramidal cells and interneurons. To determine whether these inputs differ in their weights of activating GABAergic circuits, we have studied the relative proportion of pyramidal cells and interneurons among their postsynaptic targets in serial electron microscopic sections. Local axons of CA1 pyramidal cells, intracellularly labeled in vitro or in vivo, innervated a relatively high proportion of interneuronal postsynaptic targets (65.9 and 53.8%, in vitro and in vivo, respectively) in stratum (str.) oriens and alveus. In contrast, axons of in vitro labeled CA3 pyramidal cells in str. oriens and str. radiatum of the CA1 area made synaptic junctions predominantly with pyramidal cell spines (92.9%). The postsynaptic targets of anterogradely labeled medial entorhinal cortical boutons in CA1 str. lacunosum-moleculare were primarily pyramidal neuron dendritic spines and shafts (90.8%). The alvear group of the entorhinal afferents, traversing str. oriens, str. pyramidale, and str. radiatum showed a higher preference for innervating GABAergic cells (21.3%), particularly in str. oriens/alveus. These data demonstrate that different glutamatergic pathways innervate CA1 GABAergic cells to different extents. The results suggest that the numerically smaller CA1 local axonal inputs together with the alvear part of the entorhinal input preferentially act on GABAergic interneurons in contrast to the CA3, or the entorhinal input in str. lacunosum-moleculare. The results highlight differences in the postsynaptic target selection of the feed-forward versus recurrent glutamatergic inputs to the CA1 and CA3 areas. © **2011 Wiley Periodicals, Inc.**

KEY WORDS: GABA; feed-forward inhibition; feed-back inhibition; dendritic spine; electron microscopy

[1] **Department of Cellular and Network Neurobiology, Institute of Experimental Medicine, Hungarian Academy of Sciences, H-1083 Budapest, Hungary;** [2] **Medical Research Council Anatomical Neuropharmacology Unit, Department of Pharmacology, University of Oxford, Oxford OX1 3TH, United Kingdom;** [3] **Center for Brain Research, Medical University Vienna, 1090 Vienna, Austria**

Grant sponsor: National Office for Research and Technology - Hungarian Scientific Research Fund (NKTH-OTKA); Grant number: CNK 77793; Grant sponsor: NIH; Grant numbers: MH54671 and NS030549; Grant sponsor: Medical Research Council, UK

*Correspondence to: Virág T. Takács, Department of Cellular and Network Neurobiology, Institute of Experimental Medicine, Hungarian Academy of Sciences, Budapest, P.O. Box 67, H-1450, Hungary. E-mail: takacs.virag@koki.hu

Received 20 April 2011Accepted for publication 21 July 2011
DOI 10.1002/hipo.20974
Published online 28 September 2011 in Wiley Online Library (wileyonlinelibrary.com).

INTRODUCTION

The hippocampal CA1 area receives abundant feed-forward excitation from several extrinsic sources as well as relatively sparse recurrent glutamatergic inputs from local pyramidal cells. The majority of the excitatory inputs derive from CA3 pyramidal cells via their ipsilateral Schaffer collaterals and contralateral commissural fibers to stratum (str.) radiatum and oriens (Schaffer, 1892; Amaral and Witter, 1989). Excitatory afferents arrive in str. lacunosum-moleculare from layer III pyramidal cells of the entorhinal cortex through the temporo-ammonic pathway (Steward and Scoville, 1976). In addition to the dense fiber bundle in str. lacunosum-moleculare that enter via the perforant pathway, a smaller number of entorhinal fibers arrive via the alveus and str. oriens and then pass through str. pyramidale and radiatum on their way to their termination zone in str. lacunosum-moleculare ["alvear pathway"(Deller et al., 1996)]. Other glutamatergic inputs arrive from the nucleus reuniens thalami (Wouterlood et al., 1990; Dolleman-Van der Weel and Witter, 2000; Bokor et al., 2002), from the perirhinal cortex (Naber et al., 1999) and from the amygdala (Pikkarainen et al., 1999). There is a dual serotonergic/glutamatergic projection from the median raphe nucleus (Varga et al., 2009) and glutamatergic inputs may originate from the medial septum as well (Colom et al., 2005; Huh et al., 2010).

The most abundant excitatory pathways to the CA1 area—the Schaffer collaterals and entorhinal fibers—innervate both pyramidal cells and interneurons (Desmond et al., 1994; Kiss et al., 1996; Wittner et al., 2006), therefore their activation is likely to evoke disynaptic feed-forward inhibition which has a pivotal role in the regulation of network activity (Buzsáki, 1984; Pouille and Scanziani, 2001; Ferrante et al., 2009; Pouille et al., 2009).

In addition to the excitation arriving from extrinsic sources, CA1 pyramidal cells themselves have sparse local collaterals, which travel in a narrow band at the border of the str. oriens and the alveus (Ramon y Cajal, 1911; Lorente de No, 1934, Knowles and

Schwartzkroin, 1981a; Tamamaki et al., 1987; Tamamaki and Nojyo, 1990) and were shown to innervate both local pyramidal cells (Deuchars and Thomson, 1996) and interneurons (Buhl et al., 1994). These interneurons might be responsible for the observed strong recurrent inhibition (Andersen et al., 1963). In vitro paired recordings of CA1 pyramidal cells and their putative targets revealed a higher yield of innervated interneurons than of local pyramidal cells (Knowles and Schwartzkroin, 1981b; Lacaille et al., 1987; Deuchars and Thomson, 1996; Ali and Thomson, 1998; Ali et al., 1998). These data suggest a preference for innervating interneurons similar to that observed in the case of certain subcortical pathways to the hippocampus (Freund and Antal, 1988; Freund and Gulyas, 1997) and interneuron-selective hippocampal GABAergic cells (Acsády et al., 1996; Gulyás et al., 1996). Indeed, the narrow termination area of CA1 local axons in str. oriens and alveus contains several interneuron types with horizontally oriented dendrites receiving many synapses from local pyramidal cells (Blasco-Ibanez and Freund, 1995), suited for feed-back regulation of the CA1 network (Maccaferri, 2005). Due to the spatial organization of glutamatergic fibers and GABAergic cell groups in hippocampal layers described above, different interneuron populations could be connected and preferentially influenced by feed-forward and feed-back pathways (Freund and Buzsaki, 1996; Wierenga and Wadman, 2003) and thus have distinct roles in network activity (Klausberger and Somogyi, 2008).

The implementation of realistic computational models of the CA1 network is essential for an understanding of neuronal operations in the hippocampus. This requires quantitative information on the synaptic relations of the participant cells. Therefore, we have examined the relative proportions of pyramidal and GABAergic cell targets of the three major glutamatergic inputs of the CA1 area using serial section electron microscopy. We have found that the feed-back input from local axons of CA1 pyramidal cells preferentially innervates interneurons whereas the two feed-forward glutamatergic pathways—the Schaffer collateral system and the temporo-ammonic pathway—target mostly pyramidal cells. In addition, the entorhinal projection showed layer-specific target selection, that is, the synaptic boutons of the alvear pathway outside str. lacunosum-moleculare innervated interneurons in a larger proportion than did the synaptic boutons of the entorhinal axons in str. lacunosum-moleculare.

MATERIALS AND METHODS

All procedures involving experimental animals were performed in accordance with the Animals (Scientific Procedures) Act, 1986 (UK) and associated regulations.

In Vitro Intracellular Labeling

Recording and neuronal labeling was carried out by Txema Sanz as part of his postgraduate studies at the University of Oxford under the supervision of the late Eberhard H. Buhl. Female Wistar rats (Charles River, UK; >110 g, $n = 6$) were anesthetized by inhalation of isoflurane followed by intramuscular injection of ketamine (100 mg/kg) and xylazine (10 mg/kg) and perfused transcardially with ice cold artificial cerebrospinal fluid (ACSF). The normal ACSF was composed of (in mM): 126 NaCl, 3 KCl, 1.25 NaH_2PO_4, 24 $NaHCO_3$, 2 $MgSO_4$, 2 $CaCl_2$, and 10 mM glucose. During the perfusion, cutting and recovery period NaCl was replaced by equiosmolar sucrose (256 mM), to prevent passive chloride entry, which has been suggested to be responsible for neurotoxicity during slice preparation (Aghajanian and Rasmussen, 1989). The brain was removed into chilled ACSF and 450 μm thick slices were cut with a vibroslice (Campden Instruments, UK) in the horizontal plane. Slices were then transferred to a recording chamber, where they were maintained at 33–35°C on a nylon mesh at the interface between oxygenated ACSF and a humidified atmosphere saturated with 95% O_2 and 5% CO_2. After a recovery period of 1 h, pyramidal neurons were intracellularly recorded and labeled in the CA1 or in the CA3a area using sharp microelectrodes filled with biocytin (Sigma, 2% in 1.5 M KCH_3SO_4). Pyramidal cells were recognized by their characteristic physiological parameters, such as broad action potentials, depolarizing and/or late hyperpolarizing after potentials, and spike frequency adaptation. For fixation, slices were sandwiched between two filters papers and placed overnight in a fixative containing 2.5% paraformaldehyde, 15% (v/v) saturated picric acid, and 1.25% glutaraldehyde in 0.1 M phosphate buffer (PB; pH 7.4). The slices were cryoprotected sequentially in 10 and 20% sucrose solutions and freeze-thawed over liquid nitrogen to facilitate the penetration of reagents. The slices were embedded in 10% gelatin and resectioned with a vibratome at a thickness of 60 μm. Sections were incubated overnight in avidin–biotinylated horseradish peroxidase complex [ABC; Vector; 1% in Tris-buffered Saline, (TBS; 0.05 M, pH 7.4)] and labeled cells were visualized by a peroxidase reaction developed with 3,3′-diaminobenzidine tetrahydrochloride [DAB, 0.05% in Tris buffer (pH 7.6)] as chromogen and 0.01% H_2O_2 as substrate.

In Vivo Juxtacellular Labeling

Male Sprague–Dawley rats ($n = 4$; 250–350 g) were anaesthetized with 1.25 g/kg urethane, plus supplemental doses of ketamine and xylazine (20 and 2 mg/kg, respectively) as needed; body temperature was maintained with a heating pad. Neuronal activity in the hippocampus was recorded extracellularly with a glass electrode filled with 1.5% neurobiotin in 0.5 M NaCl. The extracellularly recorded cells were individually labeled with neurobiotin using the juxtacellular labeling method by applying positive current steps (Pinault, 1996). Two to four hours after labeling, cardiac perfusion with saline was followed by ~20 min fixation with a fixative of 4% paraformaldehyde, 15% (v/v) saturated picric acid, and 0.05% glutaraldehyde in 0.1 M PB. The brains were dissected and cut transversely into 70 μm-thick serial sections. The visualization of neurobiotin

was carried out by avidin-biotinylated horseradish peroxidase method using DAB as chromogen and glucose oxidase generated H_2O_2 (Itoh et al., 1979).

Anterograde Tracing

The anterograde labeling experiments were carried out by Txema Sanz as part of his postgraduate studies at the University of Oxford under the supervision of P.S. During deep sodium pentobarbitone anesthesia (intraperitoneal injection, 220 mg/kg) the anterograde tracer Phaseolus vulgaris leucoagglutinin (PHAL, 2.5% in 0.01 M PB, Vector, Peterborough, UK) was delivered into layers II/III of the medial entorhinal cortex of female Wistar rats (Charles River, UK; >110 g, $n = 3$) through glass micropipettes by applying a 7–8 μA positive pulsed current at a cycle of 7 seconds on/7 seconds off, for 15 minutes. Injection sites were selected according to the atlas of Paxinos and Watson (1998): left hemisphere, AP (from Interaural Line): 2.28 mm and 0.7 mm; L: 4.6 mm; DV: 7.6 mm and 5.8 mm. After a survival period of 7–10 days, the rats were deeply reanaesthetized (as above) and perfused transcardially with saline for 1 min, followed by a fixative containing 4% (animal 3) or 0.5% paraformaldehyde (animals 1 and 2), 15% (v/v) saturated picric acid and 0.05% (animal 3), or 2.5% glutaraldehyde (animals 1 and 2) in 0.1 M PB. Blocks of the left hemisphere were cryoprotected sequentially by 10 and 20% sucrose, and freeze-thawed in liquid nitrogen. Serial horizontal sections (70 μm thick) were cut on a vibratome, and incubated in a blocking solution containing 20% normal goat serum (Vector) in TBS for 1 hour. PHAL labeling was visualized using a biotinylated goat antibody against PHAL (Vector, 1:1000 in TBS, 2 days at 4°C), followed by 1% ABC in TBS for 3 hours and a peroxidase reaction developed with DAB.

Tissue Processing for Electron Microscopy

The sections were treated with osmium (1 or 2% OsO4, 40 min in PB), dehydrated in an ascending ethanol series followed by propylene oxide and flat embedded in Durcupan (ACM, Fluka). Either before or during dehydration, the sections were treated with 1% uranyl acetate (30 min).

Electron Microscopic Analysis of Postsynaptic Targets of CA1 and CA3 Pyramidal Cells

The axonal arbors of in vivo or in vitro filled CA1 and CA3 pyramidal cells were reconstructed using a drawing tube at 100× magnification. Characteristic axon collaterals were photographed, re-embedded, serially sectioned using an ultramicrotome (Leica, Wien, Austria) and analyzed with correlated light and electron microscopy. Long series of consecutive ultrathin sections (60 or 70 nm thick) were collected on Formvar-coated single-slot grids and counterstained with lead citrate (Ultrostain 2, Leica). Labeled axons were traced in serial ultrathin sections and all synapses found were photographed using a Philips CM 410 electron microscope or a Hitachi 7100 electron microscope equipped with a Veleta CCD camera (Olympus Soft Imaging Solutions, Germany). The postsynaptic target was followed in consecutive serial sections and its nature was determined using published criteria (Gulyás et al., 1999; Megías et al., 2001). Briefly, in str. radiatum, pyramidale, and oriens of the CA1 area, pyramidal cells receive type 1 synapses on their dendritic spines, but not on their dendritic shafts, which are innervated almost exclusively by type 2 synapses. In contrast, interneurons receive type 1 synapses mostly on their dendritic shafts. Therefore, dendritic shafts innervated by labeled axons were considered to originate from interneurons if they received type 1 inputs. Dendritic spines were identified by their size and specific shape emerging from a dendrite. Most pyramidal cell spines have characteristic head and neck and only one type 1 input (Megías et al., 2001). So-called sessile spines having a stubby head without a neck are rare (Kirov et al., 1999). Although most hippocampal interneurons are essentially aspinous (Freund and Buzsaki, 1996), in CA1 str. oriens/alveus the dendrites of many types can be spiny (Baude et al., 1993; Blasco-Ibanez and Freund, 1995). These spines can be innervated by more than one type 1 input (Takács et al., 2008). To distinguish between interneuron and pyramidal spines in these layers, spines with only one input were followed to their parent dendrites. It was not possible to decide if some small postsynaptic profiles, which could not be followed in sufficient serial sections were spines or small dendritic shafts and these were labeled as unidentified.

A random sample of nine postsynaptic dendritic shafts predicted to originate from GABAergic neurons based on their synaptic input alone were tested for the presence of GABA immunoreactivity using a postembedding immunogold method and the same antiserum to GABA as published earlier (Somogyi and Hodgson, 1985). The density of colloidal gold particles over all of these dendrites, particularly over mitochondria, was significantly greater than that over presumed pyramidal cell dendrites, which did not receive type 1 inputs on their dendritic shafts (Mann-Whitney U test, $P < 0.0005$). This result confirmed that the identification of dendritic shafts based on synaptic input alone, as originating from interneurons or pyramidal cells, is robust, which allowed us to sample a large population of postsynaptic targets.

Electron Microscopic Analysis of Postsynaptic Targets of Entorhinal Axons

Due to the different densities of PHAL-labeled fibers, synaptic contacts made by the entorhinal axons in str. lacunosum-moleculare and outside of str. lacunosum-moleculare were sampled in different ways. In the alveus, str. oriens, pyramidale, and radiatum relatively few labeled axons could be seen, therefore, these were analyzed with correlated light and electron microscopy, similarly to the collaterals of the CA1 and CA3 pyramidal cells (see above). Individual axonal segments were traced in serial sections and all synapses found were photographed and included in the sample. In str. lacunosum-moleculare, a much denser fiber labeling was achieved and therefore, instead of reconstructing individual axonal segments, we used a

systematic random sampling technique. Blocks of CA1 str. lacunosum-moleculare were re-embedded and serially sectioned at ~60 nm thickness using an ultramicrotome. Pairs of consecutive serial sections (reference section and look-up section) were randomly selected. The reference section was systematically scanned for synapses formed by labeled boutons. In accordance with the disector principle (Sterio, 1984), synapses contained only in the reference section were counted, while those also present in the look-up section were excluded. The postsynaptic profiles were traced in serial sections and their nature was determined as above. Because in str. lacunosum-moleculare the shafts of pyramidal dendrites may receive type 1 inputs (Megías et al., 2001), these were distinguished from interneuron dendritic shafts by the presence of spines.

Statistical Analysis

A X^2 test for heterogeneity was used to compare the frequency of pyramidal cells versus GABAergic interneuron targets among animals and input pathways. For statistical comparisons, shaft and spine targets within the pyramidal and GABAergic groups were pooled. Unidentified targets were not included in the statistical analysis.

RESULTS

Postsynaptic targets of the labeled glutamatergic pathways were analyzed in serial electron microscopic sections and classified as pyramidal cell or interneuronal elements according to the characteristic of their synaptic inputs as described in the Methods (see also Gulyás et al., 1999; Megías et al., 2001).

CA1 Pyramidal Cell Recurrent Collaterals Preferentially Target Interneurons

Single or multiple pyramidal cells were labeled in vitro and in vivo in str. pyramidale of the CA1 area. The labeled cells had axons ramifying in the subiculum and in str. oriens of the CA1 area, where they were mostly restricted close to the border of the alveus (Fig. 1A), as described earlier (Ramon y Cajal, 1911; Lorente de No, 1934; Knowles and Schwartzkroin, 1981a; Tamamaki et al., 1987; Tamamaki and Nojyo, 1990). To determine the proportions of interneuronal and pyramidal cell targets of these recurrent axons in CA1, correlated light and electron microscopy was carried out. The sampled boutons of the in vitro filled cells ($n = 41$ synapses; $n = 2$ animals and cells) innervated a high proportion of interneuronal targets (pooled total, 65.9%; 63.4% interneuron dendritic shafts, Fig. 1B; 2.4% interneuron spines) and a smaller percentage innervated pyramidal cells (29.3% pyramidal cell spines, Fig. 1C). Some (4.9%) postsynaptic targets remained unidentified. The target distributions of the two in vitro labeled cells were not significantly different from each other ($X^2 = 0$; $P = 1$).

It has been demonstrated that slice preparation can alter the number of spines and synapses (Kirov et al., 1999, 2004; Bourne et al., 2007). Because this might have had an effect on the target distribution of axons too, we examined an additional sample of CA1 recurrent synapses, formed by the labeled axons of in vivo juxtacellularly labeled CA1 pyramidal cells ($n = 130$ synapses, $n = 4$ animals, and $n = 1, 1, 2$, and 4 cells/animal). The targets of these cells were similarly distributed as those in the slices ($X^2 = 1.159$; $P = 0.259$): labeled boutons targeted 53.8% interneuronal profiles (pooled, 46.2% interneuron shaft and 7.7% interneuron spines: Fig. 1D), 39.2% pyramidal cells (37.7% pyramidal spines and 1.5% pyramidal shaft), and 6.9% of the postsynaptic profiles could not be classified. Of the 125 boutons collected, 5 (4%) made synaptic junctions with two post-synaptic elements, and these were both pyramidal spines ($n = 1$), or both interneuron shafts ($n = 1$) or a pyramidal spine and an interneuronal shaft ($n = 2$) or a pyramidal spine and an unidentified target ($n = 1$). Many of the interneuronal dendrites resembled dendrites of horizontal interneurons in str. oriens/alveus (Baude et al., 1993; Takács et al., 2008); they received a very large number of type 1 inputs on their shafts and frequently had spines covered with type 1 synapses. It is important to note that the target distribution of the in vivo labeled CA1 pyramidal cells were heterogeneous ($X^2 = 27.965$; $P < 0.0001$; Table 1).

Schaffer Collaterals Predominantly Innervate Pyramidal Cells

The CA3a pyramidal cells intracellularly labeled in vitro ($n = 4$ rats and cells) had axons that ramified extensively in the CA3 region and also projected to CA1 str. oriens (Fig. 2A) and radiatum via their Schaffer collaterals. Postsynaptic targets of the Schaffer collaterals were examined by correlated light and electron microscopy. Of the 70 synapses collected ($n = 46$ from str. oriens/alveus and $n = 24$ from str. radiatum), only 7.1% were on dendritic shafts of interneurons (Fig. 2D) and 92.9% were on pyramidal cell dendritic spines (pooled, Fig. 2B,C). Seven of the labeled boutons (11.1%) had two postsynaptic targets (Fig. 2C), which were always two dendritic spines. The target distributions of the examined population of CA3 pyramidal cells were not significantly different from each other ($X^2 = 3.02$; $P = 0.2209$).

Layer Specific Differential Synaptic Target Selection by Entorhinal Fibers

To visualize the temporo-ammonic axons innervating the CA1 area, the anterograde tracer, PHAL was injected into the medial entorhinal cortex. Light microscopic assessment of the injection sites showed that the PHAL deposit was restricted to the medial entorhinal cortex and involved mostly the superficial layers. As previously described in detail, the perforant pathway has several anatomically and functionally different components, arising from distinct subfields and layers of the entorhinal cortex (Steward, 1976; Amaral and Witter, 1989; Witter et al., 2000; van Strien et al., 2009). The termination pattern of the

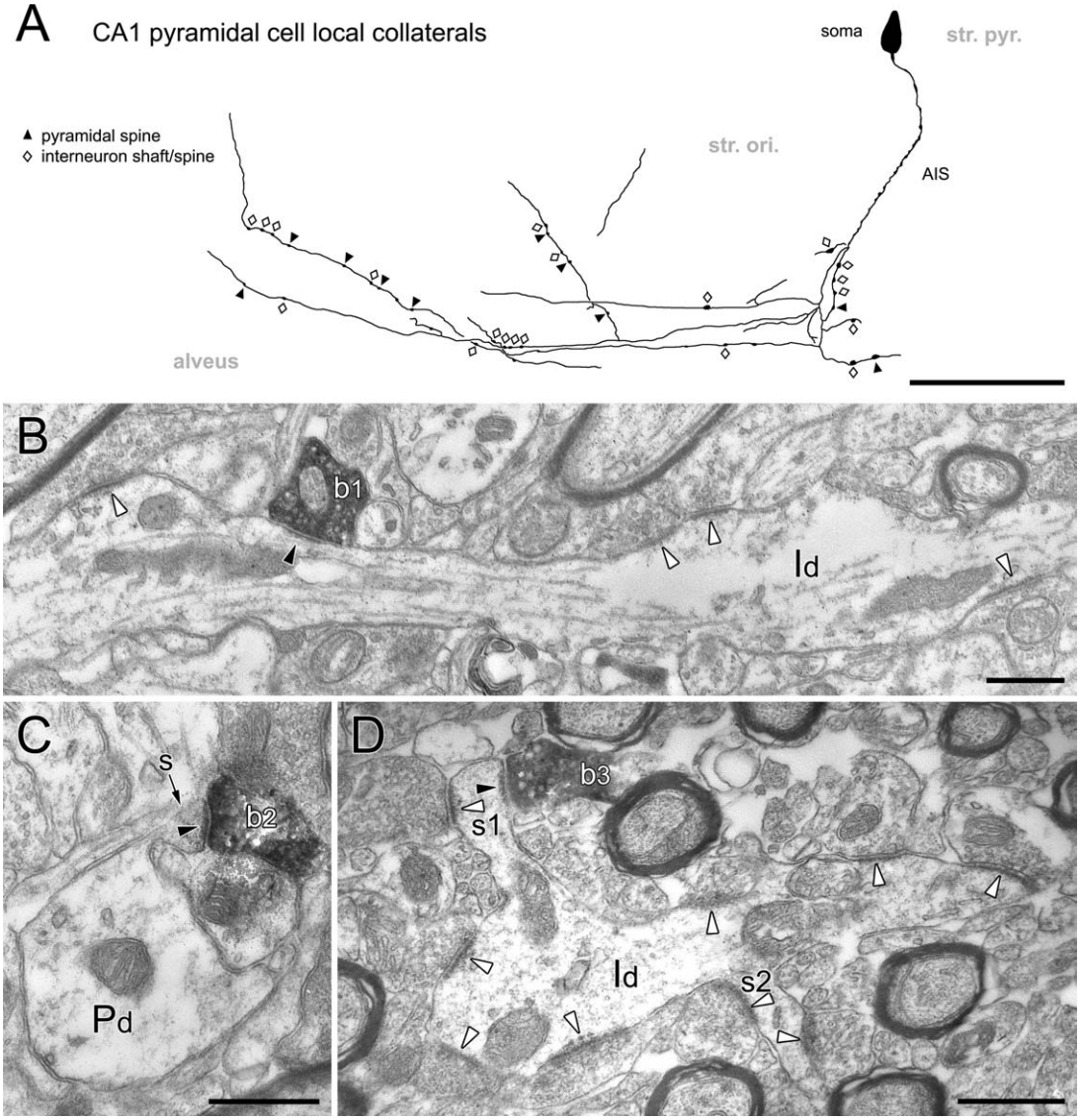

FIGURE 1. Recurrent collaterals of CA1 pyramidal cells preferentially innervate interneurons. A: Partial drawing of an in vitro labeled CA1 pyramidal cell axon, which was studied for its postsynaptic targets by electron microscopy. Arrowheads denote axonal varicosities, which were found to form synaptic junctions with pyramidal cell spines. Open diamond symbols label axon terminals, which innervated interneuronal dendritic shafts or spines. B: An axon terminal of a biocytin-filled CA1 pyramidal cell (b1) forms a type 1 synapse (black arrowhead) with the dendritic shaft of an interneuron (Id) in CA1 str. oriens. The interneuronal shaft was identified by its additional type 1 synapses (white arrowheads). C: A biocytin-labeled bouton (b2) innervates a dendritic spine (s; arrowhead) which is continuous with the shaft (Pd) of a presumed pyramidal cell. Note the lack of type 1 synaptic input to the pyramidal dendritic shaft. D: Spines of interneurons were also found postsynaptic to CA1 pyramidal cell axons. A neurobiotin-labeled axon terminal (b3) targets an interneuronal spine (s1; black arrowhead), which receives an additional type 1 synapse (white arrowhead). The spine is continuous with the shaft of the interneuronal dendrite, which emits an additional spine (s2) and receives further type 1 inputs (white arrowheads). AIS: axon initial segment, str. pyr.: stratum pyramidale, str. ori.: stratum oriens. Scale bars: A: 100 µm; B, C, and D: 0.5 µm.

labeled axons following tracer injection into the medial entorhinal cortex in this study was consistent with that reported earlier. Briefly, the majority of fibers terminated in the middle third of the molecular layer of the dentate gyrus, the inner half of str. lacunosum-moleculare of CA3 area, and str. lacunosum-moleculare of the proximal portion of CA1 (i.e., close to CA2), throughout the width of the layer. In accordance with the report by Deller et al., (1996) two pathways of entorhinal fibers to the CA1 area could be observed: (i) most of the fibers perforated the subiculum, entered str. lacunosum-moleculare of the CA1 area and formed a dense termination area in the proximal CA1 and (ii) the other, much smaller group of fibers, forming the alvear path (Deller et al., 1996), entered the angular bundle, traveled through the alveus until it was located opposite the dense termination field in str. lacunosum-moleculare of the proximal CA1 and then turned, radially traversed str. oriens, pyramidale, radiatum, and joined the former group of fibers in str. lacunosum-moleculare. On their way, these collat-

TABLE 1.

Target Distribution of all Sampled Glutamatergic Inputs to CA1 Area

Pathway (labeling)	Animal no. (*n* of labeled cells/animal)	Layer(s)	No. of synapses tested	Postsynaptic targets						
				Pyramidal cell			Interneuron			Unidentified
				Shaft	Spine	Total (% of all)	Shaft	Spine	Total (% of all)	*n* (% of all)
CA1 pyramidal cell local collaterals (in vitro)	11/07/95 (1)	s.o./alveus	31	1	8	9 (29)	21	0	21 (67.7)	1 (3.2)
	14/01/93 (1)	s.o./alveus	10	0	3	3 (30)	5	1	6 (60)	1 (10)
CA1 pyramidal cell local collaterals (in vivo)	C13 (2)	s.o./alveus	34	1	6	7 (20.6)	20	5	25 (73.5)	2 (5.9)
	C14 (4)	s.o./alveus	58	0	34	34 (58.6)	17	1	18 (31)	6 (10.3)
	J82 (1)	s.o./alveus	19	0	1	1 (5.3)	15	3	18 (94.7)	0
	J68 (1)	s.o./alveus	19	1	8	9 (47.4)	8	1	9 (47.4)	1 (5.3)
Schaffer collaterals (in vitro)	11/07/96 (1)	s.o.	37	0	35	35 (94.6)	2	0	2 (5.4)	0
	21/08/96 (1)	s.o.	6	0	6	6 (100)	0	0	0	0
	07/08/96 (1)	s.o./alveus	3	0	2	2	1	0	1	0
	26/02/97 (1)	s.r.	24	1	21	22 (91.7)	2	0	2 (8.3)	0
Entorhinal axons in s.l.-m. (in vivo)	Animal 1[a]	s.l.-m.	48	1	44	45 (93.8)	3	0	3 (6.3)	0
	Animal 2[a]	s.l.-m.	46	2	41	43 (93.5)	3	0	3 (6.5)	0
	Animal 3[a]	s.l.-m.	36	0	30	30 (83.3)	5	0	5 (13.9)	1 (2.8)
Entorhinal axons-Alvear pathway (in vivo)	Animal 1[a]	s.r.	5	0	5	5 (100)	0	0	0	0
		s.p.	14	0	14	14 (100)	0	0	0	0
		s.o./alveus	30	0	21	21 (70)	9	0	9 (30)	0
		Total 1	49	0	40	40 (81.6)	9	0	9 (18.4)	0
	Animal 2[a]	s.r.	18	0	13	13 (72.2)	5	0	5 (27.8)	0
		s.p.	16	0	16	16 (100)	0	0	0	0
		s.o./alveus	19	0	12	12 (63.2)	6	1	7 (36.8)	0
		Total 2	53	0	41	41 (77.4)	11	1	12 (22.6)	0
	Animal 3[a]	s.r.	18	0	14	14 (77.8)	4	0	4 (22.2)	0
		s.o./alveus	7	0	5	5 (71.4)	2	0	2 (28.6)	0
		Total 3	25	0	19	19 (76)	6	0	6 (24)	0

s.l.-m., stratum lacunosum-moleculare; s.o., stratum oriens; s.p., stratum pyramidale; s.r., stratum radiatum.[a]Bulk labeling of entorhinal axons.

erals also formed branches and varicosities in layers outside str. lacunosum-moleculare.

To establish whether the two groups differ in their innervation, electron microscopy was performed on temporo-ammonic axons in str. lacunosum-moleculare of the proximal CA1 as well as on alvear path fibers traversing str. oriens/alveus, pyramidale, and radiatum. Randomly sampled temporo-ammonic boutons in str. lacunosum-moleculare ($n = 130$ synapses; three animals) innervated only a small proportion of interneuronal targets (pooled, 8.5% interneuron shaft; Fig. 3Bi,ii). The vast majority of postsynaptic targets were made up of pyramidal cell spines (88.5%; Fig. 3Ai,ii) and a small proportion was pyramidal cell dendritic shafts (2.3%, Fig. 3C). One innervated dendritic shaft could not be classified (0.8%). In agreement with the results of Desmond et al., (1994), the labeled boutons established exclusively type 1 synapses. The three animals were not significantly different with regard to the postsynaptic elements of labeled entorhinal axons in str. lacunosum-moleculare ($X^2 = 2.044$; $P = 0.3598$).

Correlated light- and electron microscopic analysis of the labeled alvear path axons in layers outside str. lacunosum-moleculare ($n = 127$ synapses; $n = 56$, 30, and 41 from str. oriens/alveus, str. pyramidale, and str. radiatum, respectively; $n = 3$ rats) revealed that they formed type 1 synapses with interneurons (pooled, interneuron shafts: 20.5%, Fig. 3D; interneuron spines: 0.8%) significantly more frequently, than did entorhinal axons in str. lacunosum-moleculare ($X^2 = 7.232$; $P = 0.0048$). Pyramidal cell spines constituted 78.7% of the targets of the alvear axons (Fig. 3E). No pyramidal cell dendritic shaft target was observed outside str. lacunosum-moleculare in agreement with the results of Megías et al. (2001). The three animals were not heterogeneous based on the postsynaptic elements of the alvear pathway ($X^2 = 0.417$; $P = 0.8116$).

Statistical Comparison of the Postsynaptic Target Selection of Different Glutamatergic Pathways to CA1 Area

Statistical analysis revealed that the pooled population of CA1 pyramidal cell recurrent collaterals innervated a significantly higher proportion of interneurons (56.7% of all targets),

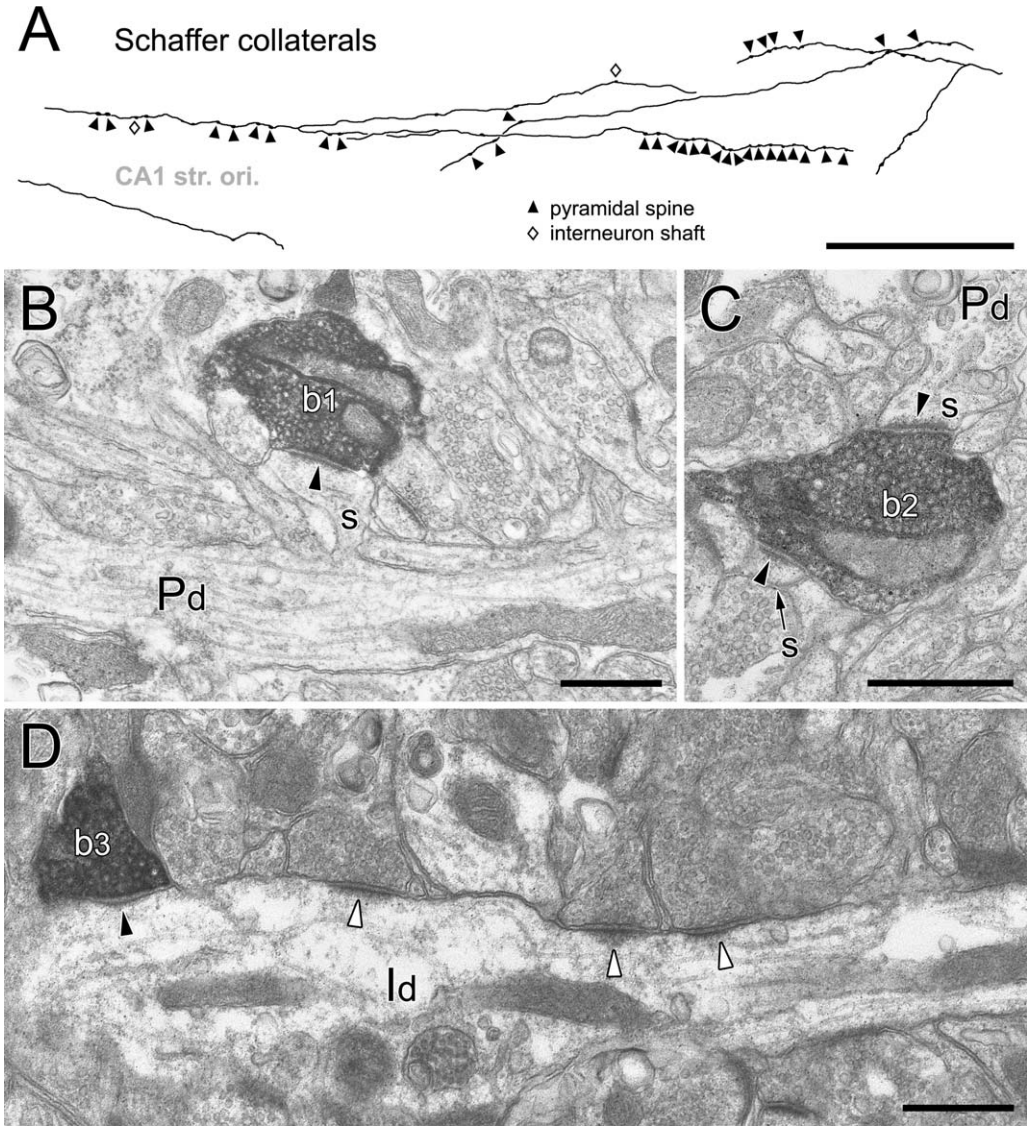

FIGURE 2. Schaffer collaterals innervate predominantly dendritic spines of pyramidal neurons. A: Partial drawing of an in vitro labeled CA3 pyramidal cell axon in stratum oriens, which was studied for its postsynaptic targets by electron microscopy. Arrowheads denote axonal varicosities, which formed synaptic junctions with pyramidal cell spines. Open diamond symbols mark axon terminals, which innervated interneuronal dendritic shafts. B: An axon terminal of a biocytin-filled CA3 pyramidal cell (b1) forms a type 1 synapse with a spine (s) of a pyramidal cell dendrite (Pd) in the CA1 str. oriens. Note the lack of type 1 synaptic input to the pyramidal dendritic shaft. C: A biocytin-filled bouton (b2) makes type 1 synaptic junctions (arrowheads) with two spines (s, arrow), one of which is continuous with the shaft of the pyramidal dendrite (Pd). D: An interneuronal dendritic shaft (Id) is postsynaptic (black arrowhead) to a labeled CA3 pyramidal cell bouton (b3). The interneuron shaft was identified by its additional type 1 synapses (white arrowheads). Str. ori.: stratum oriens. Scale bars: A: 100 μm; B, C, and D: 0.5 μm.

than the other three examined pathways (i.e., CA3 pyramidal cell axons, entorhinal axons in str. lacunosum-moleculare, and the alvear pathway; Table 2), which innervated a much higher proportion of pyramidal cell targets (Fig. 4). The entorhinal alvear pathway also innervated significantly higher percentage of interneuron targets (21.3%) than the entorhinal axons in str. lacunosum-moleculare (8.5%) or the Schaffer collaterals (7.1%). The proportions of targets of entorhinal axons in str. lacunosum-moleculare and the CA3 pyramidal cell in str. radiatum and oriens were not statistically different.

DISCUSSION

We have found that the three major glutamatergic pathways to the CA1 area exhibit remarkable differences in the relative proportion of innervated GABAergic and glutamatergic neurons. Feed-forward inputs to str. lacunosum-moleculare from the medial entorhinal cortex (temporo-ammonic pathway) and to str. radiatum and oriens from CA3 pyramidal cells (Schaffer collaterals) appear to select their postsynaptic elements in a ratio that is similar to the ratio for pyramidal/GABAergic neu-

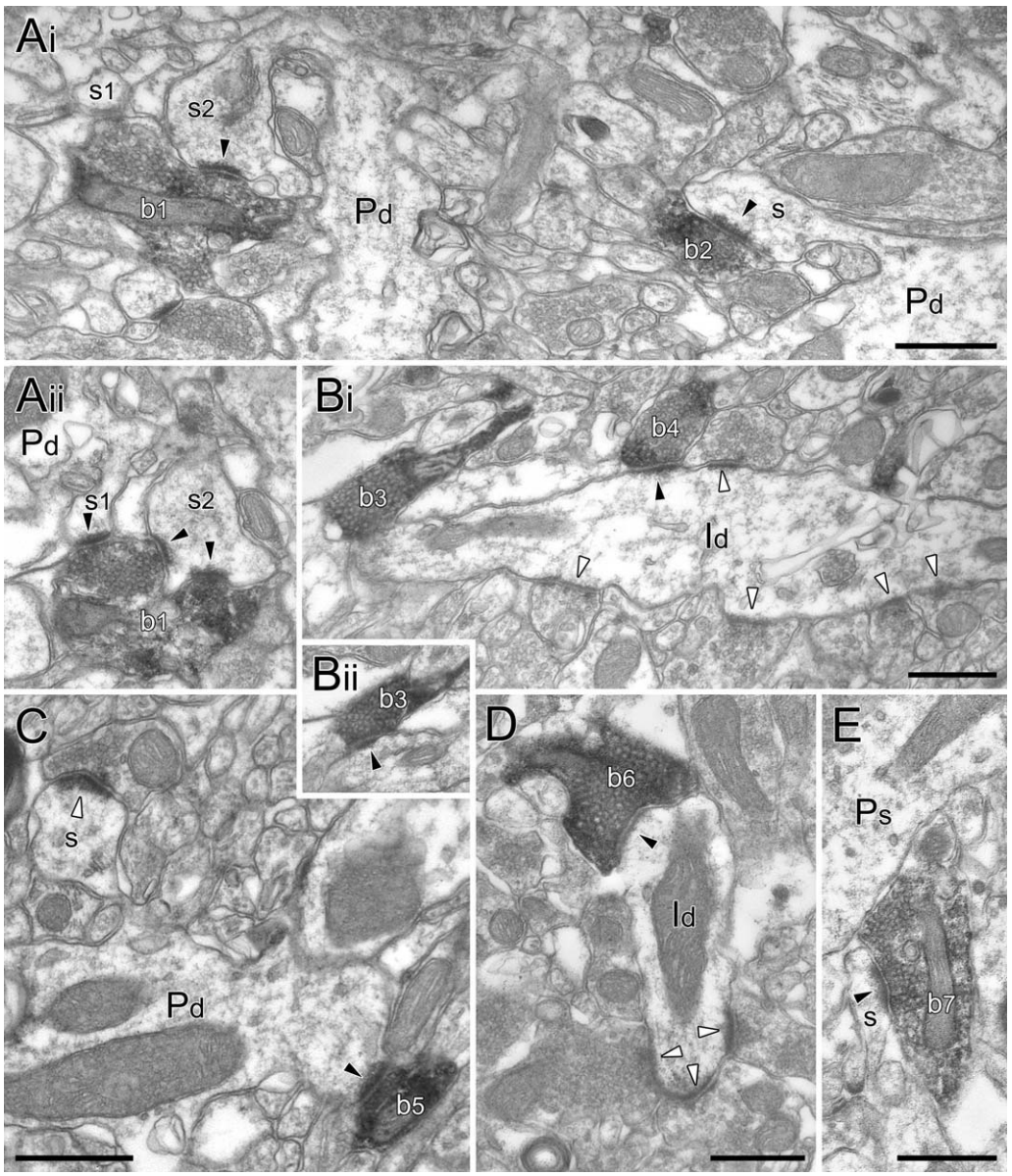

FIGURE 3. Entorhinal axons show different target selectivity in CA1 str. lacunosum-moleculare (A–C) and outside str. lacunosum moleculare ("alvear pathway," D and E). Ai,ii: Postsynaptic targets of entorhinal axons are predominantly pyramidal spines in str. lacunosum-moleculare. Ai: Two PHAL-labeled boutons (b1 and b2) form type 1 synapses (arrowheads) with spines (s and s2) emerging from pyramidal cell dendrites (Pd). Aii: The bouton b1 shown in Ai forms an additional synapse with another spine (s1, shown also in Ai) of a presumed pyramidal cell dendrite (Pd), as revealed in consecutive serial sections. The synapse formed by bouton b1 with the spine s2 is perforated (arrowheads). Bi,ii: Dendritic shafts of interneurons (Id) were less frequently innervated. B1: An interneuronal dendritic shaft is innervated by a labeled entorhinal axon terminal (b4; black arrowhead). The interneuronal dendritic shaft was identified by its abundant convergent inputs (white arrowheads) and lack of spines. Bii: The labeled bouton b3 (shown also in Bi) forms a synapse (arrowhead) with the same dendritic shaft (Id in Bi) in the next consecutive section. C: Occasionally, pyramidal cell dendritic shafts were also targeted by entorhinal terminals. The pyramidal cell dendritic shaft (Pd) receives a type 1 synapse (black arrowhead) from a labeled bouton (b5). The postsynaptic shaft was identified as a pyramidal dendrite by the lack of other inputs on its shaft and its emerging spine (s), which receives a type 1 synapse from an unlabeled terminal (white arrowhead). D and E: Entorhinal axons outside str. lacunosum-moleculare (alvear pathway) frequently innervate interneurons. D: An interneuronal dendritic shaft (Id) is innervated by a labeled entorhinal bouton (b6) with a type 1 synapse (black arrowhead) in str. oriens. Note the other convergent type 1 inputs (white arrowheads) onto the shaft. E: A labeled terminal of an alvear axon (b7) forms a type 1 synapse (arrowhead) with a spine (s) in str. pyramidale. Next to the bouton, a small part of a pyramidal cell soma is visible (Ps). Scale bars: 0.5 μm.

rons in the CA1 area [i.e., a large number of synapses to pyramidal cell (>90%) vs. few synapses to interneurons (<10%)]. In contrast, the feedback input from the local collaterals of CA1 pyramidal cells in str. oriens innervates more interneuronal elements (>50%) than expected from the ratio of pyramidal/GABAergic neurons in CA1 and the overall distri-

TABLE 2.

Statistical Comparison of the Postsynaptic Target Distribution of Different Glutamatergic Inputs to the CA1 Area

Glutamatergic pathways	CA1 pyramidal cells	Schaffer collaterals	Entorhinal axons (s. l.-m.)
Schaffer collaterals	X^2 = **54.289, P < 0.0001**		
Entorhinal axons (s. l.-m.)	X^2 = **80.619, P < 0.0001**	X^2 = 0.9431, P = 0.7928	
Entorhinal axons (alvear)	X^2 = **43.127, P < 0.0001**	X^2 = **5.618, P = 0.0092**	X^2 = **7.232, P = 0.0048**

Statistically significant differences are indicated by bold letters. S. l.-m.: stratum lacunosum-moleculare.

bution of glutamatergic synapses. In addition, the postsynaptic targets of the alvear entorhinal path fibers passing through str. oriens, pyramidale, and radiatum appear to be biased towards targeting interneurons as compared with the fibers in str. lacunosum-moleculare. These data demonstrate that no a priori assumptions can be made for the synaptic selectivity of glutamatergic axonal terminations without direct measurements.

The Recurrent Collaterals of CA1 Pyramidal Cells are Strongly Biased for Targeting Interneurons

The in vitro samples and the pooled in vitro-in vivo samples proved to be statistically homogenous; however, the in vivo sample alone did not represent a homogenous target distribution. This may reflect the expected heterogeneity of CA1 pyramidal cells, which can be subdivided into more groups according to the expression of calbindin (Baimbridge and Miller, 1982), the ability of firing complex spike bursts (Jensen et al., 1996; Jarsky et al., 2008), and their firing properties during gamma oscillations in awake rats (Senior et al., 2008). Because cells analyzed in this study were filled randomly and the sample number is relatively low, the contribution of "non-average" pyramidal cells is not known.

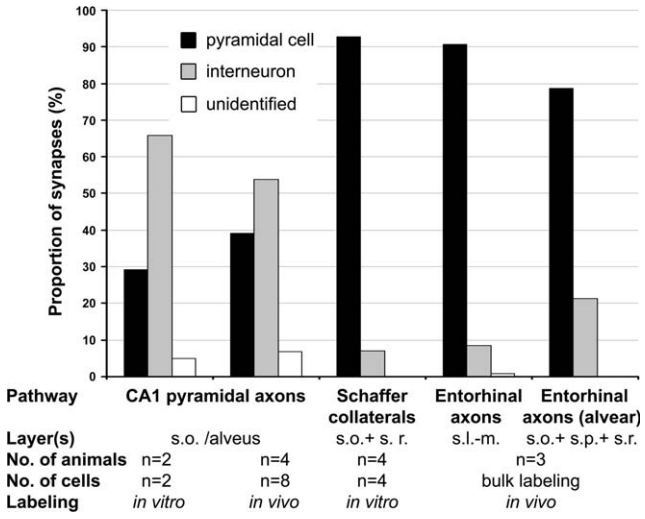

FIGURE 4. Cumulative synaptic target distribution of the three major glutamatergic inputs to the CA1 area. The pooled proportion (%) of pyramidal (black) and interneuronal synaptic targets (gray) of in vitro and in vivo labeled CA1 pyramidal cell local collaterals, in vitro filled Schaffer collaterals and entorhinal axons labeled in vivo with the anterograde tracer PHAL in str. lacunosum-moleculare and outside str. lacunosum-moleculare (alvear pathway). The proportion of unidentified targets is shown as white columns. s.l-m.: stratum lacunosum-moleculare, s.o.: stratum oriens, s.p.: stratum pyramidale, s.r.: stratum radiatum.

In the hippocampus, interneurons are less abundant than pyramidal cells [11% (Woodson et al., 1989), 7% (Aika et al., 1994)] and the number of glutamatergic inputs converging onto individual CA1 interneurons is lower than that onto pyramidal cells [1,700 – 19,000 vs. 30,000 (Gulyás et al., 1999; Megías et al., 2001; Mátyás et al., 2004; Takács et al., 2008)]. The length and distribution of interneuron dendrites and their synaptic coverage is highly non-uniform amongst cell types as shown in the above studies. Therefore, we have not attempted to estimate the overall proportion of interneuron vs. pyramidal cell targets.

From the examined pathways, CA1 pyramidal axons and entorhinal axons outside str. lacunosum-moleculare targeted a surprisingly high proportion of interneuronal elements. The pyramidal cells in the CA1 area have relatively sparse axon collaterals, which occupy a narrow layer at the border of str. oriens and the alveus (Ramon y Cajal, 1911; Lorente de No, 1934, Knowles and Schwartzkroin, 1981a; Tamamaki et al., 1987; Tamamaki and Nojyo, 1990; Biró et al., 2005). Although GAD-positive cell bodies are relatively evenly distributed in CA1 (Babb et al., 1988; Aika et al., 1994; Shi et al., 2004; Stanley and Shetty, 2004), the number of potential postsynaptic interneuronal elements at str. oriens/alveus border is probably higher than in other layers, because this area contains many types of interneuron with horizontal dendritic arbors which form a dense plexus of dendrites here (Woodson et al., 1989; Fukuda and Kosaka, 2000; Biró et al., 2005; reviewed in Maccaferri, 2005). The preferential distribution of pyramidal axon collaterals in the alveus and adjoining str. oriens rather than in the full depth of this layer, suggests that the interneuronal postsynaptic targets anchor them in and close to the alveus. In contrast, CA3 pyramidal axons innervated a much smaller percentage of interneurons in str. oriens (compare Figs. 1A and 2A) and are more evenly spread, largely sparing the alveus, where there are few if any pyramidal cell dendrites.

Many str. oriens/alveus horizontal interneurons, including the O-LM cells, express mGluR1α (Martin et al., 1992; Baude et al., 1993; Hampson et al., 1994), and carry spines on their dendrites. These cells were shown to receive a large proportion of their glutamatergic input (>70%) from CA1 pyramidal cells

(Blasco-Ibanez and Freund, 1995). Our sample also contained many labeled CA1 pyramidal cell boutons forming synapses with dendritic shafts and spines of spiny interneurons of str. oriens/alveus confirming the previous report (Blasco-Ibanez and Freund, 1995). The preferential innervation of interneurons shown here can explain the low yield of connected CA1 pyramidal cells [<1% probability (Knowles and Schwartzkroin, 1981b; Deuchars and Thomson, 1996)] compared to pyramidal cell-to-interneuron pairs [>32% probability (Knowles and Schwartzkroin, 1981b; Lacaille et al., 1987; Ali and Thomson, 1998)] in simultaneous paired intracellular recordings. However, the percentage of pyramidal cell spine targets found in our electron microscopic sample (29.3% in vitro and 39.2% in vivo) is still significant. This suggests, that the effect of some fraction of these electrotonically distal synapses on basal dendrites of pyramidal cells may be difficult to detect in somatic recordings (Lacaille et al., 1987).

During theta oscillations, there is a surprisingly long delay between the average firing of CA1 pyramidal cells and the average activity of their main afferent inputs in the CA3 area and entorhinal cortex. The peak firing of CA1 pyramidal cells follows the peak firing of CA3 pyramidal cells by about a quarter of a theta cycle and by about a half of a theta cycle the firing of the layer III entorhinal pyramidal cells (Mizuseki et al., 2009). This suggests that theta oscillations dynamics allows for a considerable degree of independence of local CA1 circuit computation, rather than monosynaptically imposing a rapidly propagating activity across regions (Mizuseki et al., 2009). Such a relatively independent organisation of theta oscillations in the CA1 area certainly requires temporal feed-back control by local GABAergic interneurons. Furthermore, CA1 interneurons, receiving strong monosynaptic input from local CA1 pyramidal cells can temporarily escape their phase locking to the field theta oscillations and together with their presynaptic pyramidal cell fire earlier on consecutive theta cycles (Maurer et al, 2006; Ego-Stengel and Wilson, 2007). Our observation that a relatively large proportion of input to local interneurons originates from CA1 pyramidal cells supports these previous reports.

Schaffer Collateral Input Innervates Pyramidal Cells and GABAergic Interneurons in the Proportions of Average Target Availability

We have found only a relatively small proportion of interneuron dendrites (7.1%) among the postsynaptic targets of in vitro labeled Schaffer collaterals as compared to the targets of CA1 pyramidal cells. Previous studies have shown that the proportion of parvalbumin- or substance P receptor- positive interneuron targets of in vivo filled CA3 pyramidal cells are 2.1 and 2.7%, respectively (Sik et al., 1993; Wittner et al., 2006). Wittner et al. (2006) also reported that CA3 pyramidal cells selectively innervate aspiny interneurons as opposed to spiny ones in the CA3 region and the hilus. The postsynaptic interneuronal dendritic shafts in the CA1 area identified in our sample also appeared to be aspiny, which might indicate that, whereas the recurrent connection from CA1 pyramidal cells involves spiny horizontal dendritic O-LM cells to a large extent (see above), the targets of Schaffer collaterals probably include mostly other types of GABAergic neurons, including basket, axo-axonic, and bistratified cells.

A strong excitatory drive from the Schaffer collateral/commissural input also initiates the generation of sharp wave-associated ripple oscillations in the CA1 area (Csicsvari et al., 2000). During these ripple events CA1 pyramidal cells have a six-fold increase in firing rate, whereas GABAergic interneurons in the CA1 area, on average across all recorded cells, increase their firing by only three-fold (Csicsvari et al., 1999). This indicates not only an overall increase of activity but also a two-fold increase in the ratio of the activity of pyramidal cells relative to all recorded interneurons. The larger fraction of pyramidal cell targets in the CA3 input as compared to the local CA1 pyramidal cell axons, may contribute to the proportionally larger increase in CA1 pyramidal cell activity relative to average interneuronal firing during sharp waves. However, there is good evidence that distinct types of interneuron are differentially activated, inhibited or do not change their activity during ripples (Klausberger and Somogyi, 2008).

Entorhinal Axons Show Different Target Selection in Different Hippocampal Layers

Entorhinal afferents in str. lacunosum-moleculare appeared to innervate their inhibitory targets in a similar ratio (8.5%) to the occurrence of GABAergic neurons to all neurons within the CA1 area [11% (Woodson et al., 1989), 7% (Aika et al., 1994)]. An earlier study demonstrated dendritic shafts thought to originate from interneurons comprised 6.5% of postsynaptic structures (Desmond et al., 1994). The postsynaptic interneurons include parvalbumin positive cells (Kiss et al., 1996), and probably many other GABAergic cell types that send dendrites to str. lacunosum-moleculare, or have most of their dendrites in this layer, such as the neurogliaform cells (Price et al., 2005). In contrast to str. lacunosum-moleculare, a higher proportion of interneuron dendrites are preferentially innervated by the alvear pathway axons outside this layer (21.3%). In vivo and in vitro electrical stimulation experiments have demonstrated that the entorhinal input activates a strong feed-forward inhibition (Colbert and Levy, 1992; Empson and Heinemann, 1995; Paré and Llinás, 1995; Soltesz, 1995; Ang et al., 2005), which, due to the high incidence of interneuron innervation by the alvear pathway, can be mediated also by interneurons with dendrites in layers other than str. lacunosum-moleculare. Fibers of the alvear pathway might even innervate the O-LM cells, which contribute to the feed-back control of the temporoammonic inputs on the distal dendrites of CA1 pyramidal cells (Maccaferri and McBain, 1995; Yanovsky et al., 1997; Maccaferri et al., 2000). The relative contribution of the alvear pathway to the entorhinal projection is not known (Deller et al., 1996), and we could not evaluate the postsynaptic targets of this pathway within str. lacunosum-moleculare due to the dense labeling of this layer.

A synchronization of gamma oscillations has been reported between the entorhinal cortex and the CA1 area of the hippocampus (Colgin et al., 2009). Amongst the interneurons innervated by entorhinal fibers, neurogliaform cells may not receive recurrent inhibition from local CA1 pyramidal cells. The spikes of neurogliaform cells are strongly correlated in time with gamma oscillations in the local extracellular field (Fuentealba et al., 2010). Taken together with our results, this suggests that input from the entorhinal cortex may contribute to synchronizing pyramidal and neurogliaform cell activity in the gamma frequency range.

Differences in the Synaptic Organization of the CA3 and CA1 Areas

The extent and the proportion of GABAergic interneuronal synaptic targets of two main input pathways to the CA3 area, the mossy fibers and the recurrent associational axon collaterals, have been studied earlier (Sik et al., 1993; Acsády et al., 1998; Wittner et al., 2006; reviewed in Acsády and Kali, 2007). Light microscopic observations suggest that the target selection of CA3 pyramidal cell axon collaterals might be similar in the CA1 and CA3 region (Sik et al., 1993; Wittner et al., 2006), suggesting that pyramidal cell associational collaterals in the CA3 area innervate a higher proportion of pyramidal cell spines than the CA1 pyramidal cell recurrent axons. In contrast to CA3 pyramidal cell axons, the intrinsic CA1 recurrent axons are sparse, provide low divergence input to pyramidal cells, and a highly divergent input to interneurons (Blasco-Ibanez and Freund, 1995; this study).

Overall, our results indicate a source-dependant target selection by distinct glutamatergic inputs to CA1 pyramidal cells and GABAergic interneurons. Such a proportioned input distribution may have evolved to generate complex neuronal computations in time across different network states. It will be interesting to explore if the source pyramidal neurons of these glutamatergic afferents show similar or different target selectivities in the other cortical areas, such as the CA3 region, the entorhinal cortex or the subiculum, which they innervate.

Acknowledgments

The authors thank Drs. Txema Sanz, Catherine Bleasdale, John Tukker and the late Dr. Eberhard Buhl for their contribution to some of the experiments and Dr. Yannis Dalezios for help with statistical analysis. Some of the material included formed part of the DPhil Thesis of Dr. Txema Sanz, The University of Oxford, 1997; Kristina Detzner, David Roberts, Katalin Lengyel, Katalin Iványi, and Győző Goda provided excellent technical assistance.

REFERENCES

Acsády L, Káli S. 2007. Models, structure, function: the transformation of cortical signals in the dentate gyrus. Prog Brain Res 163:577–599.

Acsády L, Görcs TJ, Freund TF. 1996. Different populations of vasoactive intestinal polypeptide-immunoreactive interneurons are specialized to control pyramidal cells or interneurons in the hippocampus. Neuroscience 73:317–334.

Acsády L, Kamondi A, Sík A, Freund T, Buzsáki G. 1998. GABAergic cells are the major postsynaptic targets of mossy fibers in the rat hippocampus. J Neurosci 18:3386–3403.

Aghajanian GK, Rasmussen K. 1989. Intracellular studies in the facial nucleus illustrating a simple new method for obtaining viable motoneurons in adult rat brain slices. Synapse 3:331–338.

Aika Y, Ren JQ, Kosaka K, Kosaka T. 1994. Quantitative analysis of GABA-like-immunoreactive and parvalbumin-containing neurons in the CA1 region of the rat hippocampus using a stereological method, the disector. Exp Brain Res 99:267–276.

Ali AB, Thomson AM. 1998. Facilitating pyramid to horizontal oriens-alveus interneurone inputs: Dual intracellular recordings in slices of rat hippocampus. J Physiol 507 (Pt 1):185–199.

Ali AB, Deuchars J, Pawelzik H, Thomson AM. 1998. CA1 pyramidal to basket and bistratified cell EPSPs: Dual intracellular recordings in rat hippocampal slices. J Physiol 507 (Pt 1):201–217.

Amaral DG, Witter MP. 1989. The three-dimensional organization of the hippocampal formation: A review of anatomical data. Neuroscience 31:571–591.

Andersen P, Eccles JC, Loyning Y. 1963. Recurrent inhibition in the hippocampus with identification of the inhibitory cell and its synapses. Nature 198:540–542.

Ang CW, Carlson GC, Coulter DA. 2005. Hippocampal CA1 circuitry dynamically gates direct cortical inputs preferentially at theta frequencies. J Neurosci 25:9567–9580.

Babb TL, Pretorius JK, Kupfer WR, Brown WJ. 1988. Distribution of glutamate-decarboxylase-immunoreactive neurons and synapses in the rat and monkey hippocampus: Light and electron microscopy. J Comp Neurol 278:121–138.

Baimbridge KG, Miller JJ. 1982. Immunohistochemical localization of calcium-binding protein in the cerebellum, hippocampal formation and olfactory bulb of the rat. Brain Res 245:223–229.

Baude A, Nusser Z, Roberts JD, Mulvihill E, McIlhinney RA, Somogyi P. 1993. The metabotropic glutamate receptor (mGluR1 alpha) is concentrated at perisynaptic membrane of neuronal subpopulations as detected by immunogold reaction. Neuron 11:771–787.

Biró AA, Holderith NB, Nusser Z. 2005. Quantal size is independent of the release probability at hippocampal excitatory synapses. J Neurosci 25:223–232.

Blasco-Ibáñez JM, Freund TF. 1995. Synaptic input of horizontal interneurons in stratum oriens of the hippocampal CA1 subfield: Structural basis of feed-back activation. Eur J Neurosci 7:2170–2180.

Bokor H, Csáki A, Kocsis K, Kiss J. 2002. Cellular architecture of the nucleus reuniens thalami and its putative aspartatergic/glutamatergic projection to the hippocampus and medial septum in the rat. Eur J Neurosci 16:1227–1239.

Bourne JN, Kirov SA, Sorra KE, Harris KM. 2007. Warmer preparation of hippocampal slices prevents synapse proliferation that might obscure LTP-related structural plasticity. Neuropharmacology 52:55–59.

Buhl EH, Halasy K, Somogyi P. 1994. Diverse sources of hippocampal unitary inhibitory postsynaptic potentials and the number of synaptic release sites. Nature 368:823–828.

Buzsáki G. 1984. Feed-forward inhibition in the hippocampal formation. Prog Neurobiol 22:131–153.

Colbert CM, Levy WB. 1992. Electrophysiological and pharmacological characterization of perforant path synapses in CA1: Mediation by glutamate receptors. J Neurophysiol 68:1–8.

Colgin LL, Denninger T, Fyhn M, Hafting T, Bonnevie T, Jensen O, Moser MB, Moser EI. 2009. Frequency of gamma oscillations routes flow of information in the hippocampus. Nature 462:353–357.

Colom LV, Castaneda MT, Reyna T, Hernandez S, Garrido-Sanabria E. 2005. Characterization of medial septal glutamatergic neurons and their projection to the hippocampus. Synapse 58:151–164.

Csicsvari J, Hirase H, Czurkó A, Mamiya A, Buzsáki G. 1999. Oscillatory coupling of hippocampal pyramidal cells and interneurons in the behaving Rat. J Neurosci 19:274–287.

Csicsvari J, Hirase H, Mamiya A, Buzsáki G. 2000. Ensemble patterns of hippocampal CA3-CA1 neurons during sharp wave-associated population events. Neuron 28:585–594.

Deller T, Adelmann G, Nitsch R, Frotscher M. 1996. The alvear pathway of the rat hippocampus. Cell Tissue Res 286:293–303.

Desmond NL, Scott CA, Jane JA, Levy WB. 1994. Ultrastructural identification of entorhinal cortical synapses in CA1 stratum lacunosum-moleculare of the rat. Hippocampus 4:594–600.

Deuchars J, Thomson AM. 1996. CA1 pyramid-pyramid connections in rat hippocampus in vitro: Dual intracellular recordings with biocytin filling. Neuroscience 74:1009–1018.

Dolleman-Van der Weel MJ, Witter MP. 2000. Nucleus reuniens thalami innervates gamma aminobutyric acid positive cells in hippocampal field CA1 of the rat. Neurosci Lett 278:145–148.

Ego-Stengel V, Wilson MA. 2007. Spatial selectivity and theta phase precession in CA1 interneurons. Hippocampus 17:161–174.

Empson RM, Heinemann U. 1995. The perforant path projection to hippocampal area CA1 in the rat hippocampal-entorhinal cortex combined slice. J Physiol 484 (Pt 3):707–720.

Ferrante M, Migliore M, Ascoli GA. 2009. Feed-forward inhibition as a buffer of the neuronal input-output relation. Proc Natl Acad Sci U S A 106:18004–18009.

Freund TF, Antal M. 1988. GABA-containing neurons in the septum control inhibitory interneurons in the hippocampus. Nature 336:170–173.

Freund TF, Buzsáki G. 1996. Interneurons of the hippocampus. Hippocampus 6:347–470.

Freund TF, Gulyás AI. 1997. Inhibitory control of GABAergic interneurons in the hippocampus. Can J Physiol Pharmacol 75:479–487.

Fuentealba P, Klausberger T, Karayannis T, Suen WY, Huck J, Tomioka R, Rockland K, Capogna M, Studer M, Morales M, and Somogyi P. 2010. Expression of COUP-TFII nuclear receptor in restricted GABAergic neuronal populations in the adult rat hippocampus. J Neurosci 30:1595–1609.

Fukuda T, Kosaka T. 2000. Gap junctions linking the dendritic network of GABAergic interneurons in the hippocampus. J Neurosci 20:1519–1528.

Gulyás AI, Hájos N, Freund TF. 1996. Interneurons containing calretinin are specialized to control other interneurons in the rat hippocampus. J Neurosci 16:3397–3411.

Gulyás AI, Megías M, Emri Z, Freund TF. 1999. Total number and ratio of excitatory and inhibitory synapses converging onto single interneurons of different types in the CA1 area of the rat hippocampus. J Neurosci 19:10082–10097.

Hampson DR, Theriault E, Huang XP, Kristensen P, Pickering DS, Franck JE, Mulvihill ER. 1994. Characterization of two alternatively spliced forms of a metabotropic glutamate receptor in the central nervous system of the rat. Neuroscience 60:325–336.

Huh CY, Goutagny R, Williams S. 2010. Glutamatergic neurons of the mouse medial septum and diagonal band of Broca synaptically drive hippocampal pyramidal cells: Relevance for hippocampal theta rhythm. J Neurosci 30:15951–15961.

Itoh K, Konishi A, Nomura S, Mizuno N, Nakamura Y, Sugimoto T. 1979. Application of coupled oxidation reaction to electron microscopic demonstration of horseradish peroxidase: Cobalt-glucose oxidase method. Brain Res 175:341–346.

Jarsky T, Mady R, Kennedy B, Spruston N. 2008. Distribution of bursting neurons in the CA1 region and the subiculum of the rat hippocampus. J Comp Neurol 506:535–547.

Jensen MS, Azouz R, Yaari Y. 1996. Spike after-depolarization and burst generation in adult rat hippocampal CA1 pyramidal cells. J Physiol 492 (Pt 1):199–210.

Kirov SA, Sorra KE, Harris KM. 1999. Slices have more synapses than perfusion-fixed hippocampus from both young and mature rats. J Neurosci 19:2876–2886.

Kirov SA, Petrak LJ, Fiala JC, Harris KM. 2004. Dendritic spines disappear with chilling but proliferate excessively upon rewarming of mature hippocampus. Neuroscience 127:69–80.

Kiss J, Buzsaki G, Morrow JS, Glantz SB, Leranth C. 1996. Entorhinal cortical innervation of parvalbumin-containing neurons (Basket and Chandelier cells) in the rat Ammon's horn. Hippocampus 6:239–246.

Klausberger T, Somogyi P. 2008. Neuronal diversity and temporal dynamics: The unity of hippocampal circuit operations. Science 321:53–57.

Knowles WD, Schwartzkroin PA. 1981a. Axonal ramifications of hippocampal Ca1 pyramidal cells. J Neurosci 1:1236–1241.

Knowles WD, Schwartzkroin PA. 1981b. Local circuit synaptic interactions in hippocampal brain slices. J Neurosci 1:318–322.

Lacaille JC, Mueller AL, Kunkel DD, Schwartzkroin PA. 1987. Local circuit interactions between oriens/alveus interneurons and CA1 pyramidal cells in hippocampal slices: electrophysiology and morphology. J Neurosci 7:1979–1993.

Lorente de No ,R. 1934. Studies on the structure of the cerebral cortex. II. Continuation of the study of the ammonic system. J Psychol Neurol 46:113–177.

Maccaferri G. 2005. Stratum oriens horizontal interneurone diversity and hippocampal network dynamics. J Physiol 562 (Pt 1):73–80.

Maccaferri G, McBain CJ. 1995. Passive propagation of LTD to stratum oriens-alveus inhibitory neurons modulates the temporoammonic input to the hippocampal CA1 region. Neuron 15:137–145.

Maccaferri G, Roberts JD, Szucs P, Cottingham CA, Somogyi P. 2000. Cell surface domain specific postsynaptic currents evoked by identified GABAergic neurones in rat hippocampus in vitro. J Physiol 524 (Pt 1):91–116.

Martin LJ, Blackstone CD, Huganir RL, Price DL. 1992. Cellular localization of a metabotropic glutamate receptor in rat brain. Neuron 9:259–270.

Mátyás F, Freund TF, Gulyás AI. 2004. Convergence of excitatory and inhibitory inputs onto CCK-containing basket cells in the CA1 area of the rat hippocampus. Eur J Neurosci 19:1243–1256.

Maurer AP, Cowen SL, Burke SN, Barnes CA, McNaughton BL. 2006. Phase precession in hippocampal interneurons showing strong functional coupling to individual pyramidal cells. J Neurosci 26:13485–13492.

Megías M, Emri Z, Freund TF, Gulyás AI. 2001. Total number and distribution of inhibitory and excitatory synapses on hippocampal CA1 pyramidal cells. Neuroscience 102:527–540.

Mizuseki K, Sirota A, Pastalkova E, Buzsáki G. 2009. Theta oscillations provide temporal windows for local circuit computation in the entorhinal-hippocampal loop. Neuron 64:267–280.

Naber PA, Witter MP, Lopez da Silva FH. 1999. Perirhinal cortex input to the hippocampus in the rat: Evidence for parallel pathways, both direct and indirect. A combined physiological and anatomical study. Eur J Neurosci 11:4119–4133.

Paré D, Llinás R. 1995. Intracellular study of direct entorhinal inputs to field CA1 in the isolated guinea pig brain in vitro. Hippocampus 5:115–119.

Paxinos G, Watson C. 1998. The rat brain in stereotaxic coordinates. New York: Academic Press.

Pikkarainen M, Rönkkö S, Savander V, Insausti R, Pitkänen A. 1999. Projections from the lateral, basal, and accessory basal nuclei of the amygdala to the hippocampal formation in rat. J Comp Neurol 403:229–260.

Pinault D. 1996. A novel single-cell staining procedure performed in vivo under electrophysiological control: Morpho-functional features of juxtacellularly labeled thalamic cells and other central neurons with biocytin or Neurobiotin. J Neurosci Methods 65:113–136.

Pouille F, Scanziani M. 2001. Enforcement of temporal fidelity in pyramidal cells by somatic feed-forward inhibition. Science 293:1159–1163.

Pouille F, Marin-Burgin A, Adesnik H, Atallah BV, Scanziani M. 2009. Input normalization by global feedforward inhibition expands cortical dynamic range. Nat Neurosci 12:1577–1585.

Price CJ, Cauli B, Kovacs ER, Kulik A, Lambolez B, Shigemoto R, Capogna M. 2005. Neurogliaform neurons form a novel inhibitory network in the hippocampal CA1 area. J Neurosci 25:6775–6786.

Ramon y Cajal ,S. 1911. Histologie du Système Nerveux de l'Homme et des Vertébrés. Maloine: Paris.

Schaffer ,K. 1892. Beitrag zur histologie der Amnionshornformation. Arch Mikrosk Anat 39:611–632.

Senior TJ, Huxter JR, Allen K, O'Neill J, Csicsvari J. 2008. Gamma oscillatory firing reveals distinct populations of pyramidal cells in the CA1 region of the hippocampus. J Neurosci 28:2274–2286.

Shi L, Argenta AE, Winseck AK, Brunso-Bechtold JK. 2004. Stereological quantification of GAD-67-immunoreactive neurons and boutons in the hippocampus of middle-aged and old Fischer 344 x Brown Norway rats. J Comp Neurol 478:282–291.

Sik A, Tamamaki N, Freund TF. 1993. Complete axon arborization of a single CA3 pyramidal cell in the rat hippocampus, and its relationship with postsynaptic parvalbumin-containing interneurons. Eur J Neurosci 5:1719–1728.

Soltesz I. 1995. Brief history of cortico-hippocampal time with a special reference to the direct entorhinal input to CA1. Hippocampus 5:120–124.

Somogyi P, Hodgson AJ. 1985. Antisera to gamma-aminobutyric acid. III. Demonstration of GABA in Golgi-impregnated neurons and in conventional electron microscopic sections of cat striate cortex. J Histochem Cytochem 33:249–257.

Stanley DP, Shetty AK. 2004. Aging in the rat hippocampus is associated with widespread reductions in the number of glutamate decarboxylase-67 positive interneurons but not interneuron degeneration. J Neurochem 89:204–216.

Sterio DC. 1984. The unbiased estimation of number and sizes of arbitrary particles using the disector. J Microsc 134 (Pt 2):127–136.

Steward O. 1976. Topographic organization of the projections from the entorhinal area to the hippocampal formation of the rat. J Comp Neurol 167:285–314.

Steward O, Scoville SA. 1976. Cells of origin of entorhinal cortical afferents to the hippocampus and fascia dentata of the rat. J Comp Neurol 169:347–370.

Takács VT, Freund TF, Gulyás AI. 2008. Types and synaptic connections of hippocampal inhibitory neurons reciprocally connected with the medial septum. Eur J Neurosci 28:148–164.

Tamamaki N, Nojyo Y. 1990. Disposition of the slab-like modules formed by axon branches originating from single CA1 pyramidal neurons in the rat hippocampus. J Comp Neurol 291:509–519.

Tamamaki N, Abe K, Nojyo Y. 1987. Columnar organization in the subiculum formed by axon branches originating from single CA1 pyramidal neurons in the rat hippocampus. Brain Res 412:156–160.

van Strien NM, Cappaert NL, Witter MP. 2009. The anatomy of memory: An interactive overview of the parahippocampal-hippocampal network. Nat Rev Neurosci 10:272–282.

Varga V, Losonczy A, Zemelman BV, Borhegyi Z, Nyiri G, Domonkos A, Hangya B, Holderith N, Magee JC, Freund TF. 2009. Fast synaptic subcortical control of hippocampal circuits. Science 326:449–453.

Wierenga CJ, Wadman WJ. 2003. Functional relation between interneuron input and population activity in the rat hippocampal cornu ammonis 1 area. Neuroscience 118:1129–1139.

Witter MP, Wouterlood FG, Naber PA, Van Haeften T. 2000. Anatomical organization of the parahippocampal-hippocampal network. Ann N Y Acad Sci 911:1–24.

Wittner L, Henze DA, Záborszky L, Buzsáki G. 2006. Hippocampal CA3 pyramidal cells selectively innervate aspiny interneurons. Eur J Neurosci 24:1286–1298.

Woodson W, Nitecka L, Ben-Ari Y. 1989. Organization of the GABAergic system in the rat hippocampal formation: A quantitative immunocytochemical study. J Comp Neurol 280:254–271.

Wouterlood FG, Saldana E, Witter MP. 1990. Projection from the nucleus reuniens thalami to the hippocampal region: Light and electron microscopic tracing study in the rat with the anterograde tracer Phaseolus vulgaris-leucoagglutinin. J Comp Neurol 296:179–203.

Yanovsky Y, Sergeeva OA, Freund TF, Haas HL. 1997. Activation of interneurons at the stratum oriens/alveus border suppresses excitatory transmission to apical dendrites in the CA1 area of the mouse hippocampus. Neuroscience 77:87–96.